Volcanic flux of nitrogen from the Earth

Article *in* Chemical Geology · January 2001

DOI: 10.1016/S0009-2541(00)00252-7

5 authors, including:

Yuji Sano
The University of Tokyo
455 PUBLICATIONS **10,772** CITATIONS
SEE PROFILE

Yoshiro Nishio
Kochi University
42 PUBLICATIONS **1,142** CITATIONS
SEE PROFILE

Tobias Fischer
University of New Mexico
234 PUBLICATIONS **6,236** CITATIONS
SEE PROFILE

Stanley Williams
Arizona State University
51 PUBLICATIONS **3,435** CITATIONS
SEE PROFILE

ELSEVIER

Chemical Geology 171 (2001) 263–271

CHEMICAL GEOLOGY
INCLUDING
ISOTOPE GEOSCIENCE

www.elsevier.com/locate/chemgeo

Volcanic flux of nitrogen from the Earth

Yuji Sano [a,*], Naoto Takahata [a], Yoshiro Nishio [b], Tobias P. Fischer [c,1], Stanley N. Williams [c]

[a] *Department of Earth and Planetary Sciences, Hiroshima University, Higashi-Hiroshima 739-8526, Japan*
[b] *Earthquake Research Institute, University of Tokyo, Tokyo 113-0032, Japan*
[c] *Department of Geology, Arizona State University, Tempe, AZ 85287-1404, USA*

Received 13 April 1999; accepted 17 March 2000

Abstract

The global flux of nitrogen from subduction zones is estimated by the elemental and isotopic compositions of nitrogen, argon and helium observed in volcanic gases and hydrothermal fluids in island arcs and in back-arc basin basalt (BABB) glasses. The $^{3}He/^{4}He$ ratios of island arc samples vary from 4.7 R_{atm} to 7.5 R_{atm}, indicating a typical subduction signature. The $^{40}Ar/^{36}Ar$ ratios are consistent with atmospheric values except for a few samples. The $\delta^{15}N$ values range from $+0.1‰$ to $+4.6‰$, which is generally higher than those of BABB glasses. Taking into account data distribution in the $\delta^{15}N–N_2/^{36}Ar$ diagram, we distinguish three nitrogen components (mantle-derived, sedimentary and atmospheric nitrogen) for the island arc samples. Contribution of mantle-derived nitrogen is 9–30% in the samples, which is consistent with that of mantle-derived carbon. It is possible to calculate nitrogen flux based on the ^{3}He flux in the literature and $N_2/^{3}He$ ratios corrected for elemental fractionation. The nitrogen flux of 6.4×10^{8} mol/year from island arc is comparable with 5.6×10^{8} mol/year from back-arc basin, but smaller than 2.2×10^{9} mol/year from mid-ocean ridges. In detail, island arcs show a large flux of subducted sedimentary nitrogen, while back-arc basins have a relatively small but measurable subduction component. The nitrogen flux of 4.1×10^{6} mol/year from hot spot region is significantly small, which is consistent with the characteristic of global carbon flux from the Earth. Total volcanic flux of nitrogen amounts to 2.8×10^{9} mol/year by taking mid-ocean ridge, hot spot and subduction values. The global nitrogen flux, if it has been constant for the 4.55 billion years of geological time, leads to an accumulation of 1.3×10^{19} mol in total, which is one order of magnitude smaller than 1.8×10^{20} mol of the present inventory of nitrogen at the Earth's surface.

Keywords: Nitrogen; Helium; Argon; Volcanic flux; Subduction zone

1. Introduction

Nitrogen has been discharging for a long time from the Earth's mantle to the atmosphere through volcanic and hydrothermal activity (Rubey, 1951). The nitrogen flux from the Earth's mantle has been estimated at mid-ocean ridges to be $1.2–3.2 \times 10^{9}$ mol/year (Marty, 1995), $1.6–6.4 \times 10^{9}$ mol/year

* Corresponding author. Earthquake Research Institute, University of Tokyo, Tokyo 113-0032, Japan. Tel.: +81-824-24-7464; fax: +81-824-24-0735.
E-mail address: ysano@ipc.hiroshima-u.ac.jp (Y. Sano).
[1] Present address: Department of Earth and Planetary Sciences, The University of New Mexico, Northrop Hall, Albuquerque, NM 87131-1116, USA.

0009-2541/01/$ - see front matter
PII: S0009-2541(00)00252-7

(Zhang and Zindler, 1993) and 8.5×10^9 mol/year (Javoy et al., 1986). However, its geochemical behavior during subduction, and therefore its recycling rate, is not well constrained. This is partly due to ambiguous signature of nitrogen isotopic compositions in mantle-derived samples. In addition, the average amount of nitrogen recycled in deep-sea sediments and subducted oceanic crust and their isotopic signatures are not well known. Recently, Marty and Humbert (1997) proposed a $\delta^{15}N$ value (where $\delta^{15}N = [(^{15}N/^{14}N)_{sample}/(^{15}N/^{14}N)_{air} - 1] \times 1000$) in the range -3 to -5‰ for the convective upper mantle, based on the correlation between $\delta^{15}N$ and $^{40}Ar/^{36}Ar$ ratios in vesicles of mid-ocean ridge basalt (MORB) glasses. Cartigny et al. (1997) have suggested that the $\delta^{15}N$ value of the sub-continental mantle is homogeneous at -5‰ to -8‰ using pristine diamond samples. Thus, considering MORB and pristine diamond data, it is currently thought that nitrogen in the Earth's upper mantle is characterized by a globally uniform $\delta^{15}N$ value of -5 ± 2‰. Based on the $\delta^{15}N$ and $N_2/^{36}Ar$ ratios of back-arc basin basalt (BABB) glasses, and using simple mixing equations, Sano et al. (1998a) have proposed quantitative estimates for the different geochemical end-members contributing to the back-arc magma source.

We report here the origin of nitrogen in volcanic gases and hydrothermal fluids in island arc and in BABB glasses based on the $N_2/^{36}Ar$ ratios and $\delta^{15}N$ values. We further discuss igneous flux of nitrogen from island arc and back-arc basin by using $N_2/^3He$ ratios and $\delta^{15}N$ values. Since nitrogen may be partly lost during devolatilization processes due to the increasing metamorphism with the subducting slab, an estimated flux of nitrogen from island arc and back-arc basin may provide a constraint on the recycling rate of nitrogen. The recycling of nitrogen is fundamental to decipher among different models of atmospheric nitrogen evolution. We also present nitrogen flux from hot spot region using $N_2/^3He$ ratios of ocean island basalt (OIB) glasses and discuss the degassing model.

2. Experimental

Fresh basalt glass samples were selected by eyes to avoid atmospheric contamination. They were crushed under vacuum and extracted gases and/or small aliquots of volcanic gases and hydrothermal fluids were purified by using a high vacuum line equipped with hot CuO, hot platinum foil and a cryogenic trap. We did not specify chemical form of nitrogen such as N_2, NH_3 and NO_2. The nitrogen isotopic composition was measured by using a modified noble gas mass spectrometer (VG3600, Micromass) at Hiroshima University. Prior to isotope analysis, the amount of nitrogen was adjusted to that of standard gas, which is about 0.15 nmol, in order to compensate any pressure effect on the measurement of the isotopic ratio. The $^{15}N/^{14}N$ ratio was determined from the observed $28^+/29^+$ ratio, and calibrated against atmospheric standard gas. Contribution of $^{13}C^{16}O$ to mass 29 was negligibly small in the present samples since the $30^+/29^+$ ratios agree well with the expected $^{15}N^{15}N/^{14}N^{15}N$ ratio. The analytical error on the $\delta^{15}N$ value was less than ± 0.5‰, estimated by the reproducibility of the standard within 1 month. Accuracy of the measurement is again less than ± 0.5‰, checked by comparison of the observed $\delta^{15}N$ value in the system with the data measured by the conventional dynamic mass spectrometer. Experimental details of the nitrogen isotopic composition are given elsewhere (Takahata et al., 1998).

After nitrogen isotope measurements, the $N_2/^{40}Ar$ ratios were determined by measuring the $28^+/40^+$ ratio in the same mass spectrometer and calibrated against air standard. The $^{40}Ar/^{36}Ar$ and $^4He/^{40}Ar$ ratios were measured by on-line quadrupole mass spectrometry (Massmate100, ULVAC) after purification using a hot Ti getter and a cryogenic trap. The $^3He/^4He$ ratios were analyzed by a conventional noble gas mass spectrometer (6-60-SGA, Nuclide) installed at Hiroshima University, after purification using hot Ti–Zr getters and activated charcoal traps held at liquid nitrogen temperature. Observed $^3He/^4He$ ratios were calibrated against atmospheric standard gas. Experimental details including accuracy and precision of helium analysis are given elsewhere (Sano and Wakita, 1985).

3. Results

Table 1 lists $\delta^{15}N$ values, $^{40}Ar/^{36}Ar$ ratios and $N_2/^{36}Ar$ ratios together with a few data from the

Table 1
$\delta^{15}N$, $N_2/^{36}Ar$ and $^{40}Ar/^{36}Ar$ ratios of ocean island basalt, back-arc basin basalt and volcanic gases in island arc

Sample	Location	$\delta^{15}N$ (‰)	$N_2/^{36}Ar$	$^{40}Ar/^{36}Ar$	Nitrogen component (A)[a]		
					Air	Mantle	Sediment
Ocean island basalt (OIB) glass							
KH85-4-D17-DE51	Loihi, HI	−0.4	2.49×10^4	360	72.0%	19.6%	8.4%
KH85-4-D17-DE55-1	Loihi, HI	0.4	5.42×10^4	669	33.0%	35.8%	31.3%
KH85-4-D17-DE55-3	Loihi, HI	0.4	2.98×10^4	369	60.2%	20.0%	19.8%
Back-arc basin basalt (BABB) glass							
KT84-1-24-1[b]	Mariana Trough	−1.9	2.09×10^5	1780	8.3%	69.5%	22.2%
KT84-1-24-2[b]	Mariana Trough	1.9	3.67×10^4	391	48.5%	13.9%	37.6%
KT84-1-24-3[b]	Mariana Trough	−2.7	6.63×10^4	619	26.8%	65.3%	7.8%
ST4-DV17-3[b]	North Fiji Basin	−1.1	6.78×10^4	352	26.2%	52.1%	21.8%
ST4-DV19-1[b]	North Fiji Basin	0.4	7.15×10^5	2020	2.2%	53.5%	44.3%
ST4-DV21-5[b]	North Fiji Basin	1.8	2.99×10^4	362	59.8%	8.1%	32.1%
ST14-DT7-2	North Fiji Basin	1.6	1.50×10^6	4320	0.9%	44.5%	54.6%
295-R-02	Manus Basin	−0.6	3.58×10^4	306	50.0%	34.1%	15.8%
303-R-02	Manus Basin	0	2.60×10^4	302	69.0%	18.1%	12.9%
Volcanic gas and hydrothermal fluid in island arc (IA)							
Kudriavy-1, 187°C	Kamchatka	2.8[c]	5.08×10^4	297	35.2%	14.9%	49.9%
Kudriavy-2, 920°C	Kamchatka	3.7[c]	9.57×10^4	302	18.5%	17.1%	64.4%
Tangkuban, 95°C	Indonesia	0.1	3.75×10^4	309	47.8%	30.1%	22.2%
Merapi Woro, 575°C	Indonesia	1.5	3.08×10^4	309	21.4%	19.6%	59.0%
Papandayan, 334°C	Indonesia	4.0	9.11×10^4	300	19.5%	14.0%	66.5%
Kamojang, 90°C	Indonesia	1.1	2.59×10^4	295	69.3%	8.9%	21.8%
Dieng Sikidang, 94°C	Indonesia	0.9	4.33×10^4	294	41.3%	26.6%	32.1%
Dieng Pakuwaja, 91°C	Indonesia	0.1	2.51×10^4	298	71.5%	15.9%	12.6%
Galeras Crater, 218°C	Colombia	3.2	7.00×10^4	314	25.4%	16.5%	58.1%
Purace, 200°C	Colombia	3.3	9.42×10^4	300	18.8%	20.3%	60.9%
Colima, 340°C	Mexico	4.6	9.72×10^4	334	18.2%	9.6%	72.1%
Component							
Air and air-saturated water		0	1.80×10^4	296	100%	0%	0%
Upper mantle		−5	6.00×10^6	64000	0%	100%	0%
Sediment		7	$> 6.00 \times 10^6$	> 300	0%	0%	100%

[a] Uncertainty: ±50%.
[b] From Sano et al. (1998a).
[c] From Fischer et al. (1998).

literature (Fischer et al., 1998; Sano et al., 1998a). The $N_2/^{36}Ar$ ratios are calculated from the observed $N_2/^{40}Ar$ and $^{40}Ar/^{36}Ar$ ratios. The $\delta^{15}N$ and $^{40}Ar/^{36}Ar$ ratios of subduction zone samples vary significantly from −2.7‰ to +4.6‰ and from 294 to 4320, respectively.

Fig. 1 shows the relationship between the $\delta^{15}N$ values and the $N_2/^{36}Ar$ ratios of the volcanic gases and hydrothermal fluids in island arc, BABB and OIB glasses together with the upper mantle, sedimentary and atmospheric end-members. There is a positive correlation between $\delta^{15}N$ values and $N_2/^{36}Ar$ ratios in volcanic gas and fluid samples, suggesting a mixing trend between air and/or air-saturated water, and a high $\delta^{15}N$–high $N_2/^{36}Ar$ component. In contrast, there is no simple relationship between the $\delta^{15}N$ and the $N_2/^{36}Ar$ in BABB glasses. The $\delta^{15}N$ values of OIB glasses are consistent with atmospheric value, while $N_2/^{36}Ar$ and $^{40}Ar/^{36}Ar$ ratios show higher values than the air. The distribution of data in the $\delta^{15}N$–$N_2/^{36}Ar$ diagram is consistent with a three-component mixing model

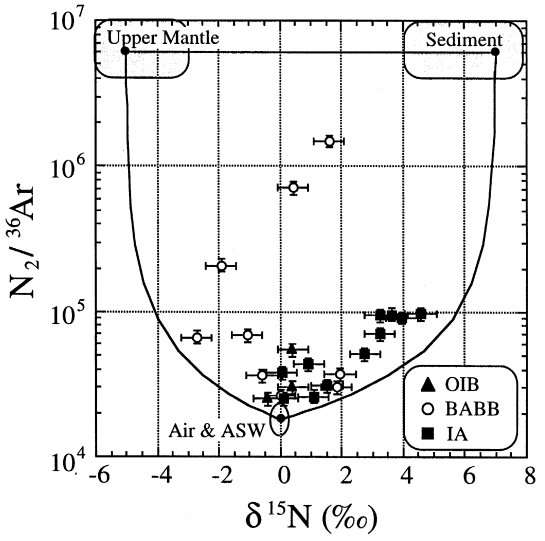

Fig. 1. A correlation diagram between $\delta^{15}N$ values and $N_2/^{36}Ar$ ratios of OIB (▲), BABB (○) and volcanic fluid in island arc, IA (■). The error assigned to the symbol is one sigma. Lines show mixing lines among the model end-members whose values are selected as follows (Sano et al., 1998a): using a $\delta^{15}N$ value of -5 ± 2‰ for the upper mantle, the mantle $N_2/^{36}Ar$ ratio of $6\pm2\times10^6$ is calculated by multiplying the uniform $N_2/^{40}Ar$ ratio of 90 ± 20 in MORB glasses (Marty and Humbert, 1997) by the highest $^{40}Ar/^{36}Ar$ ratio so far observed in MORB, $64{,}000\pm8000$ (Burnard et al., 1997). Organic nitrogen in marine sediments indicates $\delta^{15}N$ values between $+2$‰ and $+10$‰ (Peters et al., 1978) and ammonia in metasediments have the value between $+2$‰ and $+15$‰ (Bebout and Fogel, 1992). Therefore, we assume a $\delta^{15}N$ value of $+7\pm4$‰ for typical sedimentary nitrogen. The highest $N_2/^{40}Ar$ ratio of 21,000 was reported for siliceous sediment (Matsuo et al., 1978). The sedimentary $N_2/^{36}Ar$ ratio of $>6\times10^6$ is estimated by the $N_2/^{40}Ar$ ratio multiplied by the $^{40}Ar/^{36}Ar$ ratio of >300. The atmospheric $\delta^{15}N$ value is defined as 0‰ and the $N_2/^{36}Ar$ ratio of $1.8\pm0.7\times10^4$ is an average of the air $N_2/^{36}Ar$ ratio and that of air-saturated water (ASW).

(Sano et al., 1998a). If nitrogen in a sample results from mixing of air, upper mantle, and sedimentary components with masses A, M and S, respectively, then:

$$\delta^{15}N_{obs} = \delta^{15}N_{air}A + \delta^{15}N_{mantle}M + \delta^{15}N_{sed}S \quad (1)$$

$$1/(N_2/^{36}Ar)_{obs} = A/(N_2/^{36}Ar)_{air} + M/(N_2/^{36}Ar)_{mantle} + S/(N_2/^{36}Ar)_{sed} \quad (2)$$

with

$$A + M + S = 1 \quad (3)$$

where subscripts obs, air, mantle and sed refer to the observed sample, air, the upper mantle and sediment, respectively. With $\delta^{15}N_{air} = 0$‰, $\delta^{15}N_{mantle} = -5$‰, $\delta^{15}N_{sed} = +7$‰, $(N_2/^{36}Ar)_{air} = 1.8\times10^4$, $(N_2/^{36}Ar)_{mantle} = 6\times10^6$, and $(N_2/^{36}Ar)_{sed} = 6\times10^6$ (see Fig. 1), we can calculate the percentage of the three components A, M and S in the samples. In this calculation, the elemental fractionation of the $N_2/^{36}Ar$ ratio and the isotopic fractionation of the $^{15}N/^{14}N$ ratio from the source to the sampling site are not taken into account. However, the $N_2/^{36}Ar$ ratio is expected to remain constant as a gas phase separates from the basaltic melt, since the solubility of nitrogen in melt is comparable to that of argon (Marty, 1995; Miyazaki, 1996; Humbert, 1998). The $\delta^{15}N$ value may not be altered during nitrogen extraction from the source because its extraction efficiency is high and the net isotope fractionation may be compensated (Marty and Humbert, 1997). Based on the estimated range of each end-member (Matsuo et al., 1978; Peters et al., 1978; Bebout and Fogel, 1992; Burnard et al., 1997; Marty and Humbert, 1997), the overall uncertainty on the fraction is $\pm50\%$ of the original value at maximum.

The calculated contributions of each source of nitrogen by the $\delta^{15}N$–$N_2/^{36}Ar$ systematics are listed as nitrogen component (A) in Table 1. BABB glasses have about 50% mantle-derived nitrogen, except samples with low $^{40}Ar/^{36}Ar$ ratios that may display a greater contribution of surface-derived nitrogen. Volcanic gas and hydrothermal samples show a contribution of mantle-derived nitrogen of 9–30%, which is consistent with those of phenocryst in subareal volcanic rocks and fluid inclusions in hydrothermal minerals (Sano et al., 1998a). Generally, nitrogen in island arc samples is dominated by atmospheric and/or sedimentary components. Sedimentary nitrogen in the samples may be attributable to subducted marine sediment, since the major fraction of co-existing carbon is derived from the same source (Sano and Williams, 1996; Fischer et al., 1998). Contributions of atmospheric nitrogen in OIB glasses are larger than those in BABB glasses, which may reflect the relatively lower $^{40}Ar/^{36}Ar$ ratios.

Table 2 lists $^3He/^4He$, $^4He/^{40}Ar$ and $N_2/^3He$ ratios of BABB glasses and volcanic gases and hydrothermal fluids in island arc with a few data from the literature (Nishio et al., 1998; Sano et al., 1998a). The $^3He/^4He$ and $^4He/^{40}Ar$ ratios of BABB samples are apparently higher than those of island arcs. Note that $^3He/^4He$ ratios of Manus Basin show significantly higher values than those of the upper mantle, suggesting contribution of a plume-type source into the magma (Kaneoka, 1983), which is well observed in OIB samples of Table 2. The $N_2/^3He$ ratios are calculated from the observed $^3He/^4He$, $^4He/^{40}Ar$ and $N_2/^{40}Ar$ ratios. Fig. 2 shows the relation between the $\delta^{15}N$ values and the $N_2/^3He$ ratios of the volcanic gases and hydrothermal fluids in island arcs, BABB and OIB glasses together with the upper mantle, sedimentary and atmospheric end-members. The distribution of data in the $\delta^{15}N$–$N_2/^3He$ diagram is again consistent with three-component mixing, even though OIB samples may be affected by deep mantle component with more negative $\delta^{15}N$ value than those of MORB (Javoy et al., 1986). If nitrogen in a sample results from mixing of air, upper mantle, and sedimentary

Table 2
$^3He/^4He$, $^4He/^{40}Ar$ and $N_2/^3He$ ratios of ocean island basalt, back-arc basin basalt and volcanic gases in island arc

Sample	$^3He/^4He$ (R_{atm})	$^4He/^{40}Ar$	$N_2/^3He$	$N_2/^3He_{cor}$	Nitrogen component (B)[a]		
					Air	Mantle	Sediment
Ocean island basalt (OIB) glass							
KH85-4-D17-DE51	23.0	0.36	6.02×10^6	4.59×10^6	72.0%	19.6%	8.4%
KH85-4-D17-DE55-1	24.5	0.77	3.09×10^6	2.52×10^6	33.0%	35.8%	31.3%
KH85-4-D17-DE55-3	24.5	0.50	4.74×10^6	4.51×10^6	60.2%	20.0%	19.8%
Back-arc basin basalt (BABB) glass							
KT84-1-24-1	7.80[b]	11	1.16×10^6	1.29×10^6	0.0%	77.6%	22.4%
KT84-1-24-2	7.76[b]	3.4	2.69×10^6	6.49×10^6	15.0%	33.4%	51.6%
KT84-1-24-3	8.05[b]	5.9	1.55×10^6	1.38×10^6	39.1%	58.0%	2.9%
ST4-DV17-3	8.53[c]	4.5	3.82×10^6	1.73×10^6	75.0%	23.6%	1.4%
ST4-DV19-1	8.42[c]	12	2.65×10^6	1.68×10^6	35.6%	34.0%	30.4%
ST4-DV21-5	8.36[c]	30	1.37×10^7	1.11×10^7	63.1%	6.6%	30.3%
ST14-DT7-2	8.53[c]	7.8	3.75×10^6	2.02×10^6	36.1%	24.0%	40.0%
295-R-02	13.5	1.6	3.88×10^6	2.64×10^6	50.0%	34.1%	15.8%
303-R-02	13.5	1.4	3.28×10^6	4.98×10^6	69.0%	18.1%	12.9%
Volcanic gas and hydrothermal fluid in island arc (IA)							
Kudriavy-1, 187°C	6.65	0.076	2.43×10^8	6.03×10^6	60.1%	0.4%	39.6%
Kudriavy-2, 920°C	6.61	0.15	2.28×10^8	5.25×10^6	47.2%	0.4%	52.4%
Tangkuban, 95°C	7.54	0.080	1.45×10^8	2.98×10^6	98.3%	0.6%	1.1%
Merapi Woro, 575°C	6.64	0.0090	1.24×10^9	7.66×10^6	78.2%	0.1%	21.8%
Papandayan, 334°C	6.10	0.10	3.51×10^8	6.43×10^6	43.0%	0.3%	56.8%
Kamojang, 90°C	6.43	0.021	4.60×10^8	1.01×10^6	84.2%	0.2%	15.6%
Dieng Sikidang, 94°C	6.50	0.073	2.22×10^8	3.38×10^7	86.1%	0.4%	13.5%
Dieng Pakuwaja, 91°C	5.99	0.0056	1.79×10^9	5.66×10^6	98.6%	0.1%	1.3%
Galeras Crater, 218°C	6.57	0.15	1.78×10^8	3.42×10^6	52.8%	0.5%	46.6%
Purace, 200°C	6.19	0.19	1.82×10^8	4.44×10^6	52.7%	0.5%	46.8%
Colima, 340°C	4.72	0.060	7.33×10^8	9.40×10^6	34.5%	0.1%	65.4%
Component							
Air and air-saturated water	1.0	0.0004	1.1×10^{11}		100%	0%	0%
Upper mantle	8.4	9.0	8.9×10^5		0%	100%	0%
Sediment	0.02	2.0	1.4×10^5		0%	0%	100%

[a] Uncertainty: ±50%.
[b] From Sano et al. (1998b).
[c] From Nishio et al. (1998).

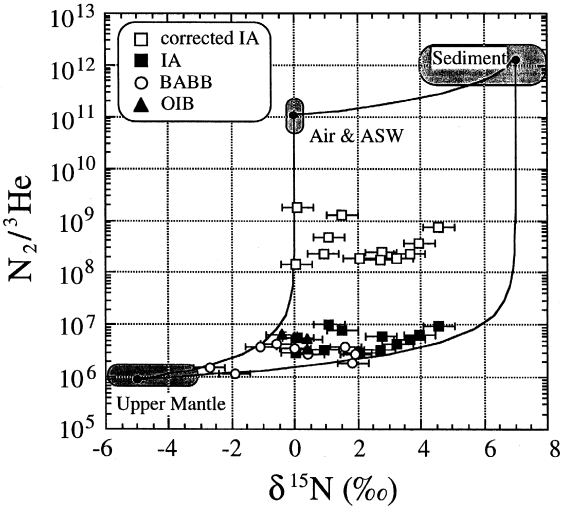

Fig. 2. A correlation diagram between $\delta^{15}N$ values and $N_2/^3He$ ratios of OIB (▲), BABB (○), volcanic fluid in island arc, IA (■) and corrected values of volcanic fluid in IA (□). The error assigned to the symbol is one sigma. Lines show mixing lines among the model end-members whose $N_2/^3He$ ratios are selected as follows: the mantle $N_2/^3He$ ratio of 8.9×10^5 is calculated by $N_2/^{40}Ar$ ratio of 90, $^4He/^{40}Ar$ ratio of 9, and $^3He/^4He$ ratio of 8.4 R_{atm} in MORB glasses (Marty, 1995). The sedimentary $N_2/^3He$ ratio of 1.4×10^{12} is estimated by N_2/Ar ratio of 21,000, radiogenic $^4He/^{40}Ar$ ratio of 2 and $^3He/^4He$ ratio of 0.02 R_{atm} (Sano and Wakita, 1985). The atmospheric $N_2/^3He$ ratio of 1.1×10^{11} is an average of the air $N_2/^3He$ and that of air-saturated water (ASW).

components with masses A, M and S, respectively, then Eq. (2) is simply replaced by the following:

$$1/(N_2/^3He)_{obs} = A/(N_2/^3He)_{air} + M/(N_2/^3He)_{mantle} + S/(N_2/^3He)_{sed} \quad (4)$$

With $(N_2/^3He)_{air} = 1.1\times10^{11}$, $(N_2/^3He)_{mantle} = 8.9\times10^5$, and $(N_2/^3He)_{sed} = 1.4\times10^{12}$ (see Fig. 2), we can again calculate the percentage of the three components A, M and S in the samples. The calculated contributions of each source of nitrogen by the $\delta^{15}N$–$N_2/^3He$ systematics are listed as nitrogen component (B) in Table 2. Taking into account the uncertainty of ±50% on each fraction, the mantle components of BABB and OIB samples are generally consistent with those estimated by the $\delta^{15}N$–$N_2/^{36}Ar$ systematics in Table 1. Note that both estimates of nitrogen components (A) and (B) on the Manus Basin and OIB samples agree with each other even though they show plume-type $^3He/^4He$ ratios. The reason of agreement is not well understood in this work. On the other hand, the mantle-derived nitrogen in volcanic gas and hydrothermal fluid is strikingly different between components (A) and (B). The discrepancy may be attributable to elemental fractionation of He and N_2 during magma degassing. Solubility of N_2 in basalt melt is identical to that of Ar (2.6×10^{-12} mol/g hPa), while it is significantly smaller than that of He (2.5×10^{-11} mol/g hPa) (Jambon et al., 1986; Marty, 1995; Miyazaki et al., 1995). Therefore, during vapor-melt separation, the N_2/Ar ratio of the exsolving gas phase will remain constant. The N_2/He ratio of vapor phase, on the other hand, is expected to decrease for the same fraction of gas exsolved from the melt, due to the higher solubility of He than Ar. This may be the reason of discrepancy between the nitrogen component (A) in Table 1 and (B) in Table 2.

In order to estimate the elemental fractionation during magma degassing, we introduce corrected $N_2/^3He$ ratios for magma that are calculated so as to make nitrogen component (B) identical to component (A) based on Eqs. (1)–(4). The observed $N_2/^3He$ ratios of BABB and OIB glasses are generally consistent with corrected ones within uncertainty of ±50%, while island arc volcanic gases show that observed ratios are about 80 times smaller values than the corrected ones. This suggests that elemental fractionation due to magma degassing is not a single step but may be in multiple stages and/or is probably affected by more complicated processes. These processes should be clarified in the future based on a complete data set of all noble gases, N_2 and CO_2. The corrected $N_2/^3He$ ratios may reflect the original signature of the magma source in an island arc volcano.

4. Discussion

We estimate the global volcanic flux of nitrogen in subduction zones based on the corrected $N_2/^3He$ ratios and ^3He flux in the literature (Torgersen, 1989). The average of the corrected $N_2/^3He$ ratios of BABB samples is 3.7×10^6, slightly smaller than

that of island arc samples, 5.6×10^6. Taking a ^{3}He flux of 7500 ± 1500 atoms/m^2 s from subduction zones (Torgersen, 1989), volcanic fluxes of nitrogen in back-arc basin and island arc amount to 7.4×10^8 mol/year and 1.12×10^9 mol/year, respectively. If we subtract the atmospheric contribution using the average of the nitrogen component (A), the fluxes become 6.4×10^8 mol/year in island arc and 5.6×10^8 mol/year in back-arc basin, respectively. Fig. 3 shows a schematic diagram of global flux of nitrogen from the Earth. Note that both back-arc basin and island arc indicate significant mantle flux of nitrogen. In detail, island arcs show a large flux of subducted sedimentary nitrogen, while back-arc basin has a relatively small but measurable subduction component.

Total length of subduction zone (continental arc and island arc) is $\sim 4 \times 10^4$ km where about 40% of the subduction is not accompanied by back-arc basin volcanism such as South and Middle America (Uyeda and Kanamori, 1979). Then, weighted mean of the nitrogen flux from subduction zones is $0.6 \times 6.4 \times 10^8$ mol/year $+ 0.4 \times 5.6 \times 10^8$ mol/year $= 6.0 \times 10^8$ mol/year, which is about 37% of the mid-ocean ridge flux. Taking the ^{3}He flux of 95 ± 5 atoms/m^2 s from hot spot regions (Torgersen, 1989) and corrected $N_2/^3$He ratios of about 3.9×10^6 observed in OIB samples with a plume-type helium and subtracting atmospheric contribution, the nitrogen flux from hot spots amounts to 4.1×10^6 mol/year, which is much smaller than that of mid-ocean ridges and subduction zones. This is consistent with the idea that the CO_2 flux from hot spots is significantly smaller than that from subduction zones (Sano and Williams, 1996). If there is an underestimate of a factor 10 for ^{3}He flux from hot spots, then the nitrogen flux is still one order of magnitude smaller than that of mid-ocean ridges and subduction zones. In order to establish the nitrogen flux from hot spots, we need more data of plume-type samples and a more precise measure of the ^{3}He flux.

Marty (1995) reported nitrogen flux from mid-ocean ridge of $2.2 \pm 1.0 \times 10^9$ mol/year that is consistent with that of $(1.6–6.4) \times 10^9$ mol/year by Zhang and Zindler (1993). Total nitrogen flux amounts to 2.8×10^9 mol/year by summing up mid-ocean ridge, hot spot and subduction values. The global nitrogen flux may account for an accumulation of 1.3×10^{19} mol in total, if the flux has been constant for the 4.55 billion years of geological time. This value is one order of magnitude smaller than 1.8×10^{20} mol of the present inventory of nitrogen at the Earth's surface (Zhang and Zindler, 1993). Recently, Tolstikhin and Marty (1998) reported the evolution of terrestrial

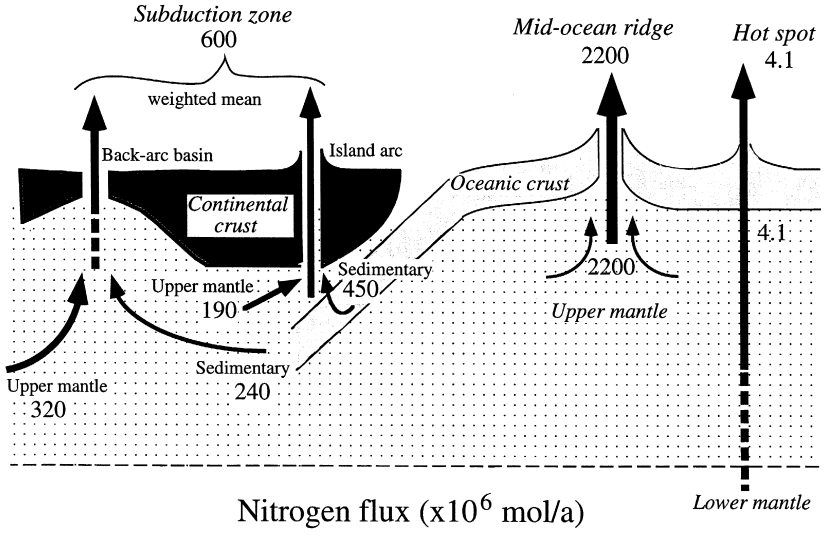

Fig. 3. A schematic diagram of nitrogen flux from the solid Earth. Note that both back-arc basin and island arc indicate significant mantle flux of nitrogen. Contribution of hot spot region is significantly smaller.

volatile where nitrogen trapped in the early Earth–Atmosphere system was depleted in ^{15}N, probably $-30‰$ and subsequently the $\delta^{15}N$ value increased to $+2.5‰$ at 4.0 Ga by atmospheric escape. Then, continuous degassing of mantle nitrogen with $\delta^{15}N$ value of $-5‰$ allowed this element to reach its present-day composition in air. Tolstikhin and Marty (1998) further suggested that the latter continuous degassing has contributed less than 3% of the present surface inventory. Taking the mantle nitrogen flux of 2.8×10^9 mol/year estimated in this work, the total nitrogen accumulated in the 4.0 billion years yields 1.1×10^{19} mol, which is about 6% of the inventory. This is comparable to that of 3% by their model when one should consider uncertainty of the flux estimate, probably factor two derived from $N_2/^3He$ variation in Table 2. Therefore, the catastrophic degassing atmosphere inferred by noble gas data in literature (Ozima, 1975; Staudacher and Allégre, 1982) may be favorable in the case of nitrogen. This is consistent with the observation of nitrogen isotopes and N_2/Ar ratios in chert samples with various formation ages, suggesting that the atmospheric $\delta^{15}N$ values has been constant over the period of 3 billion years (Sano and Pillinger, 1990). Tolstikhin and Marty (1998) reported that recycling flux of nitrogen into the upper mantle may transfer $\sim 6\%$ of surface (atmosphere + sediments) nitrogen per 1 Ga, which is about 1×10^{10} mol/year. This value is one order of magnitude larger than sedimentary nitrogen flux of 4.5×10^8 mol/year into the island arc magma source estimated in this work. The discrepancy will be discussed more precisely in the future.

5. Conclusion

We have measured the elemental and isotopic compositions of nitrogen, argon and helium in volcanic gases and hydrothermal fluids of island arc, back-arc basin basalt glasses, and ocean island basalt glasses. Isotopic compositions of helium and argon of island arc and back-arc samples show a typical subduction signature. The $^3He/^4He$ ratios of ocean island and Manus basin samples indicate plume-type value. The $N_2/^{36}Ar$ ratios and $\delta^{15}N$ value of subduction samples are well explained by mixing of three components: upper mantle, sedimentary and atmospheric nitrogen. We have estimated the nitrogen flux of 6.4×10^8 mol/year from island arc and that of 5.6×10^8 mol/year from back-arc basin based on the corrected $N_2/^3He$ ratios for elemental fractionation and ^3He flux in literature. These values are about 30% of nitrogen flux from mid-ocean ridges but significantly larger than that of 4.1×10^6 mol/year from hot spot region. Total flux of 2.8×10^9 mol/year nitrogen, if it has been constant for 4.55 billion years, would yield an accumulation of 1.3×10^{19} mol, which is still one order of magnitude smaller than 1.8×10^{20} mol of the present nitrogen inventory at the Earth's surface.

Acknowledgements

We thank Y. Tsutsumi and R. Yokochi for help in laboratory and A.P. Nutman, N.C. Sturchio and B. Marty for comments. Original manuscript was written when Y.S. was staying at Earthquake Research Institute, University of Tokyo as a visiting professor. This work was partly supported by Grant-in-Aid for scientific research program no. 0840436 from the Ministry of Education, Science and Culture of Japan. T.P.F. was partially supported by a NASA Earth System Science Graduate Fellowship during the course of this work. We thank an anonymous reviewer and E. Hauri for numerous constructive comments.

References

Bebout, G.E., Fogel, M., 1992. Nitrogen-isotope compositions of metasedimentary rocks in the Catalina Schist, California: implications for metamorphic devolatilization history. Geochim. Cosmochim. Acta 56, 2839–2849.

Burnard, P., Graham, D., Turnar, G., 1997. Vesicle-specific noble gas analyses of "popping rock": implications for primordial noble gases in earth. Science 276, 568–571.

Cartigny, P., Boyd, S.R., Harris, J.W., Javoy, M., 1997. Diamonds and the isotopic composition of mantle nitrogen. Terra Nova 9, 175–179.

Fischer, T.P., Giggenbach, W.F., Sano, Y., Williams, S.N., 1998. Fluxes and sources of volatiles from Kudryavy, a subduction zone volcano, Kurile Islands. Earth Planet. Sci. Lett. 160, 81–96.

Humbert, F., 1998. Solubilité de l'azote dans les silicates liquides. PhD Thesis, Université Henri Poincaré, Nancy I, 1998.

Jambon, A., Weber, H., Braun, O., 1986. Solubility of He, Ne, Ar, Kr and Xe in a basalt melt in the range 1250–1600°C. Geochemical implications. Geochim. Cosmochim. Acta 50, 401–408.

Javoy, M., Pineau, F., Delorme, H., 1986. Carbon and nitrogen isotopes in the mantle. Chem. Geol. 57, 41–62.

Kaneoka, I., 1983. Noble gas constraint on the layered structure of the mantle. Nature 302, 698–700.

Marty, B., 1995. Nitrogen content of the mantle inferred from N_2–Ar correlation in oceanic basalts. Nature 377, 326–329.

Marty, B., Humbert, F., 1997. Nitrogen and argon isotopes in oceanic basalts. Earth Planet. Sci. Lett. 152, 101–112.

Matsuo, S., Susuki, M., Mizutani, Y., 1978. Nitrogen to argon ratio in volcanic gases. In: Alexander, E.C., Ozima, M. (Eds.), Terrestrial Rare Gases. Center for Academic Publishing Japan, Tokyo, pp. 17–25.

Miyazaki, A., 1996. Studies on solubilities of nitrogen and noble gases in silicate melts. PhD Thesis, University of Tokyo.

Miyazaki, A., Hiyagon, H., Sugiura, N., 1995. Solubilities of nitrogen and argon in basalt melt under oxidizing conditions. In: Farley, K.A. (Ed.), Volatiles in the Earth and Solar System. pp. 276–283.

Nishio, Y., Sasaki, S., Gamo, T., Hiyagon, H., Sano, Y., 1998. Carbon and helium isotope systematics of North Fiji Basin basalt glasses: carbon geochemical cycle in the subduction zone. Earth Planet. Sci. Lett. 154, 127–138.

Ozima, M., 1975. Ar isotopes and earth–atmosphere evolution models. Geochim. Cosmochim. Acta 39, 1127–1134.

Peters, K.E., Sweeney, R.E., Kaplan, I.R., 1978. Correlation of carbon and nitrogen stable isotope ratios in sedimentary organic matter. Limnol. Oceanogr. 23, 598–604.

Rubey, W.W., 1951. Geologic history of sea water: an attempt to state the problem. Geol. Soc. Am. Bull. 62, 1111–1148.

Sano, Y., Pillinger, C.T., 1990. Nitrogen isotopes and N_2/Ar ratios in cherts: an attempt to measure time evolution of atmospheric $\delta^{15}N$ value. Geochem. J. 24, 315–325.

Sano, Y., Wakita, H., 1985. Geographical distribution of $^3He/^4He$ ratios in Japan: implications for arc tectonics and incipient magmatism. J. Geophys. Res. 90, 8729–8741.

Sano, Y., Williams, S.N., 1996. Fluxes of mantle and subducted carbon along convergent plate boundaries. Geophys. Res. Lett. 23, 2749–2752.

Sano, Y., Nishio, Y., Gamo, T., Jambon, A., Marty, B., 1998a. Noble gas and carbon isotopes in Mariana Trough basalt glasses. Appl. Geochem. 13, 441–449.

Sano, Y., Takahata, N., Nishio, Y., Marty, B., 1998b. Nitrogen recycling in subduction zones. Geophys. Res. Lett. 25, 2289–2292.

Staudacher, T., Allégre, C.J., 1982. Terrestrial xenology. Earth Planet. Sci. Lett. 60, 389–406.

Takahata, N., Nishio, Y., Yoshida, N., Sano, Y., 1998. Presice isotopic measurements of nitrogen at the sub-nanomole level. Anal. Sci. 14, 485–491.

Tolstikhin, I.N., Marty, B., 1998. The evolution of terrestrial volatiles: a view from helium, neon, argon and nitrogen isotope modelling. Chem. Geol. 147, 27–52.

Torgersen, T., 1989. Terrestrial helium degassing fluxes and the atmospheric helium budget: implications with respect to the degassing processes of continental crust. Chem. Geol. 79, 1–14.

Uyeda, S., Kanamori, H., 1979. Back-arc opening and the mode of subduction. J. Geophys. Res. 84, 1049–1061.